Multicopy plasmids allow bacteria to escape from fitness trade-offs during evolutionary innovation

Jeronimo Rodriguez-Beltran [1]*, J. Carlos R. Hernandez-Beltran[2], Javier DelaFuente[1], Jose A. Escudero[3], Ayari Fuentes-Hernandez[2], R. Craig MacLean [4], Rafael Peña-Miller[2] and Alvaro San Millan [1,5]*

Understanding the mechanisms governing innovation is a central element of evolutionary theory. Novel traits usually arise through mutations in existing genes, but trade-offs between new and ancestral protein functions are pervasive and constrain the evolution of innovation. Classical models posit that evolutionary innovation circumvents the constraints imposed by trade-offs through genetic amplifications, which provide functional redundancy. Bacterial multicopy plasmids provide a paradigmatic example of genetic amplification, yet their role in evolutionary innovation remains largely unexplored. Here, we reconstructed the evolution of a new trait encoded in a multicopy plasmid using TEM-1 β-lactamase as a model system. Through a combination of theory and experimentation, we show that multicopy plasmids promote the coexistence of ancestral and novel traits for dozens of generations, allowing bacteria to escape the evolutionary constraints imposed by trade-offs. Our results suggest that multicopy plasmids are excellent platforms for evolutionary innovation, contributing to explain their extreme abundance in bacteria.

The ability of a species to expand its ecological niche and thrive in new environments depends directly on the development of novel adaptive traits through evolutionary innovation. Evolutionary innovation, in turn, relies on the repurposing of old traits to serve new roles[1,2]. Examples of this process are abundant and include the development of important traits such as new metabolic capabilities[3], the control of bacterial division[4], and the evolution of multicellularity[5]. However, mutations providing a new role are usually detrimental to native gene function. These negative correlations between ancestral and evolved traits are called trade-offs. Trade-offs are common during evolutionary innovation and have been identified in a plethora of natural and experimental settings[2]. Crucially, the interplay between trade-offs and selective pressures for the ancestral and new activities determines the fate of innovative mutations. For instance, strong selection to maintain the native activity leads to the purging of variants with adaptive potential, hampering innovative evolution[6,7]. Hence, trade-offs are arguably one of the major constraints on evolutionary innovation.

Several models have been proposed to explain the ready occurrence of innovation despite the restraints imposed by trade-offs. Most of these models are based on the emergence of genetic amplifications that provide genetic redundancy[1,8–11]. Amplifications, such as duplications, alleviate trade-offs because they allow the coexistence of different alleles of the same gene. In this way, extra gene copies might acquire new functions while others retain their original role[8]. However, genetic amplifications might be unstable as they are usually a target for homologous recombination, resulting in the deletion of one of the duplicated regions[10,12]. Furthermore, the majority of amplifications have been found to be neutral or deleterious in the absence of selection[13]. Nevertheless, stable amplifications have been reported for genes involved in antibiotic resistance[14], metabolism[15] or encoding weak secondary functions[11,16].

Among the most paradigmatic examples of genetic mechanisms providing genetic redundancy in prokaryotes are multicopy plasmids (MCPs): small and highly prevalent genetic elements in bacteria[17], that typically range from 10 to 30 copies per cell and lack active segregation and partition systems[18]. Therefore, MCPs maintain a population of the same genes within a cell, and thus can be regarded as an extreme example of stable genetic amplification. Here, we propose that MCPs could alleviate trade-offs during the evolution of innovation. This hypothesis is based on two predictions. First, the multicopy nature of these plasmids allows different versions of the gene (alleles) to coexist in the same cell under heterozygosity, and this coexistence will alleviate fitness trade-offs. Second, once the evolved allele appears, plasmid segregation and replication dynamics will maintain heterozygosity at the cellular and population level for a prolonged period of time, even under strong selection for one of the alleles (Fig. 1a). To test these predictions, we used a well-characterized model of antibiotic resistance evolution in which trade-offs have profound effects on adaptive trajectories[7,19,20]. By combining simple mathematical models with experimental work, we demonstrate that MCPs promote the maintenance of genetic diversity against strong selection, alleviating trade-offs and promoting evolutionary innovation.

Results

Experimental system. TEM-1 is a β-lactamase that confers high-level resistance to penicillins such as ampicillin (Amp) but negligible resistance to third generation cephalosporins such as ceftazidime (Caz). The evolution of TEM-1 toward conferring Caz resistance has been shown in laboratory and natural settings to occur predominantly via a single mutation (Arg164Ser) that gives rise to TEM-12[19,21]. The evolved allele (bla_{TEM-12}) confers high-level resistance to Caz at the expense of a reduced activity against Amp compared with the ancestral allele (bla_{TEM-1}), thus demonstrating a

[1]Department of Microbiology, Hospital Universitario Ramon y Cajal (IRYCIS), Madrid, Spain. [2]Centro de Ciencias Genómicas, Universidad Nacional Autónoma de México, Morelos, Mexico. [3]Departamento de Sanidad Animal and VISAVET, Facultad de Veterinaria, Universidad Complutense de Madrid, Madrid, Spain. [4]Department of Zoology, University of Oxford, Oxford, UK. [5]Network Research Center for Epidemiology and Public Health (CIBER-ESP), Madrid, Spain. *e-mail: jeronimo.rodriguez.beltran@gmail.com; alvsanmillan@gmail.com
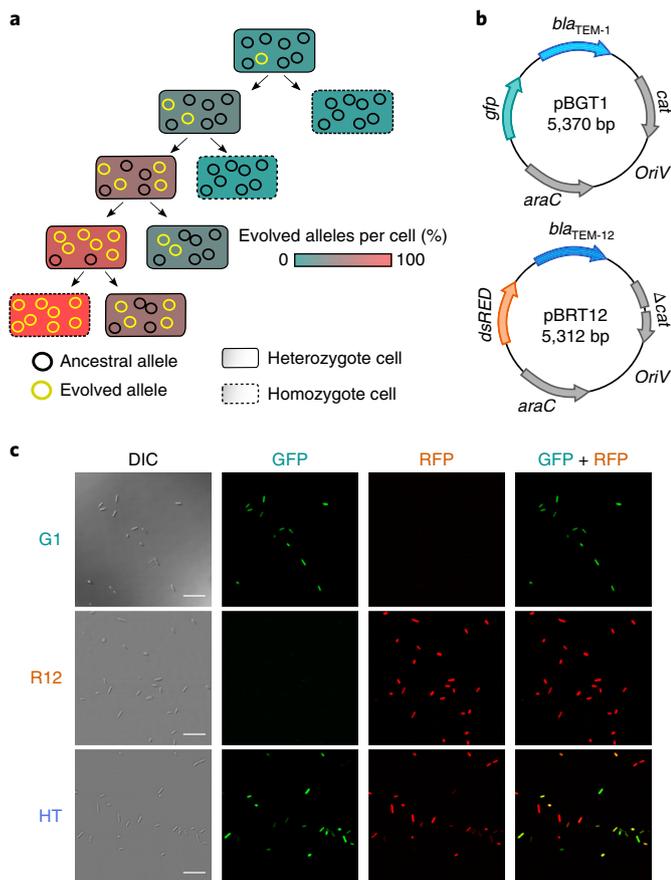
Fig. 1 | Conceptual and experimental models. a, Scheme of the plasmid replication and segregation dynamics that drive the co-existence of ancestral and mutated alleles under heterozygosity. In every generation, plasmids are randomly segregated to daughter cells and then replicated. Following this simple model, heterozygosity is maintained for several generations as an emergent property of plasmid replication and segregation dynamics. **b**, Maps of the plasmids used in our experimental model. **c**, Confocal microscopy images showing representative fields of bacterial populations of the G1 and R12 homozygote strains, and the HT strain. Scale bar, 10 µm.

trade-off between Amp and Caz resistance[19,21]. In a recent study, we detected TEM-12 mutation arising in response to Caz pressure in an experimental model using plasmid pBGT-1; an MCP carrying bla_{TEM-1} (ref. [21]). Crucially, sequencing of evolved clones revealed pBGT-1 plasmid variants differing only in the TEM Arg164 residue coexisting under heterozygosity (see supplementary file 2 of ref. [21]). To test the ability of MCPs to alleviate trade-offs, we reproduced the TEM-1 evolutionary scenario using a traceable MCP system. We developed two plasmids coding TEM-1 or TEM-12. As the ancestral allele carrier we used plasmid pBGT-1, which occurs at ~19 copies per bacterium and includes a bla_{TEM-1} gene and a tightly controlled gfp gene[21]. In parallel, we constructed the pBRT-12 plasmid by replacing bla_{TEM-1} with bla_{TEM-12} and the gfp gene with $dsRED$ to allow plasmid identification by fluorescence (Fig. 1b). We also constructed plasmids with interchanged fluorescent markers (pBGT-12 and pBRT-1; Supplementary Fig. 1) and used them to show that the reporter genes did not influence the results obtained hereafter (Supplementary Table 1, Supplementary Figs. 2–4). We transformed *Escherichia coli* MG1655 with the pBGT1 and pBRT12 plasmids individually, respectively generating the G1 and R12 strains, and also together to generate a heterozygote strain (HT) carrying both plasmids (Supplementary Table 1). Direct observation of cells under

confocal microscopy (Fig. 1c) and whole-genome sequencing of the genomes of all strains confirmed their isogenic nature and the presence of the different plasmids.

Multicopy plasmid-mediated heterozygosity alleviates trade-offs.
It is reasonable to expect that, by maintaining copies of the ancestral and the evolved alleles within individual cells, MCPs would alleviate trade-offs emerging during evolutionary innovation. To test this possibility, we measured the ability of the G1, R12 and HT strains to colonize an array of 48 liquid environments containing varying concentrations of Caz or Amp alone or in combination (Fig. 2a). We also included a 1:1 mixed population of the G1 and R12 homozygotes as a control. The G1 and R12 strains were unable to grow at high concentrations of Caz or Amp, respectively, demonstrating the anticipated trade-off (Fig. 2a). By contrast, both the HT and the mixed population colonized a significantly higher number of antibiotic environments than the ancestral (G1) and evolved (R12) strains (Fig. 2b; one-way ANOVA $F = 290.7$, d.f. = 3, $P < 0.001$ followed by Tukey's multiple comparison of means $P < 0.001$). This result indicated that the presence of both alleles, either at the population level (the mixed population) or at the cellular level (the HT strain), allowed bacterial populations to persist in the presence of Caz and Amp.

Because the plasmids used in this study were engineered to carry distinguishable fluorescence reporters (Fig. 1b), we were able to estimate the relative abundance of bla_{TEM-1} and bla_{TEM-12} alleles by simply measuring the GFP/RFP ratio in each environment (Methods and Supplementary Fig. 5). As expected, both the HT and the mixed populations—but not the homozygotes—showed variation in the plasmid proportions in every environment in response to different antibiotic combinations (Fig. 2c). In general, higher concentrations of Caz selected for higher proportions of pBRT12, biasing fluorescence toward red (Spearman's rho −0.58 and −0.71 for Mix and HT, respectively; $P < 0.01$). Higher Amp concentrations selected for pBGT1, and therefore produced a higher GFP/RFP ratio (Spearman's rho 0.92 and 0.69 for Mix and HT, respectively; $P < 0.03$).

To quantify allelic richness across environments, we counted the environments that contained both plasmids at detectable levels (that is, environments with fluorescence ratios between those of the homozygote populations; shaded region on Fig. 2d). Although the HT and Mix populations were able to colonize the same number of environments, HT maintained both alleles to a greater extent than the mixed population (45% [38/84] versus 23% [18/78] of the colonized environments, respectively; $\chi^2 = 7.8293$, d.f. = 1, $P < 0.01$).

Multicopy plasmids maintain genetic diversity against selection.
Our second prediction was that once an adaptive mutation appears in an MCP, random plasmid segregation will maintain heterozygosity at the cellular level (and consequently at the population level) for a prolonged period, even under strong selection for one of the alleles. To study the fixation dynamics of the innovative allele bla_{TEM-12} under strong Caz selective pressure, we performed invasion experiments in which a small (~1%) HT population invades a G1 population. As a control, we performed the same experiment with R12, instead of HT, invading the G1 population (Fig. 3). The experiment, which ran for eight days with four replicates per treatment, started with the minimal selective concentration[22] of Caz for the bla_{TEM-12} allele (0.0625 mg l^{-1}; Supplementary Fig. 4). Every day, 0.1% of each population was transferred to fresh medium containing double the Caz concentration of the preceding day. The relative abundance of each genotype was tracked by selective plating, and the frequency of the bla_{TEM-1} and bla_{TEM-12} alleles in every population was determined by qPCR.

The results showed that the G1 strain was rapidly outcompeted both by the R12 and HT strains at the same Caz concentration (25%
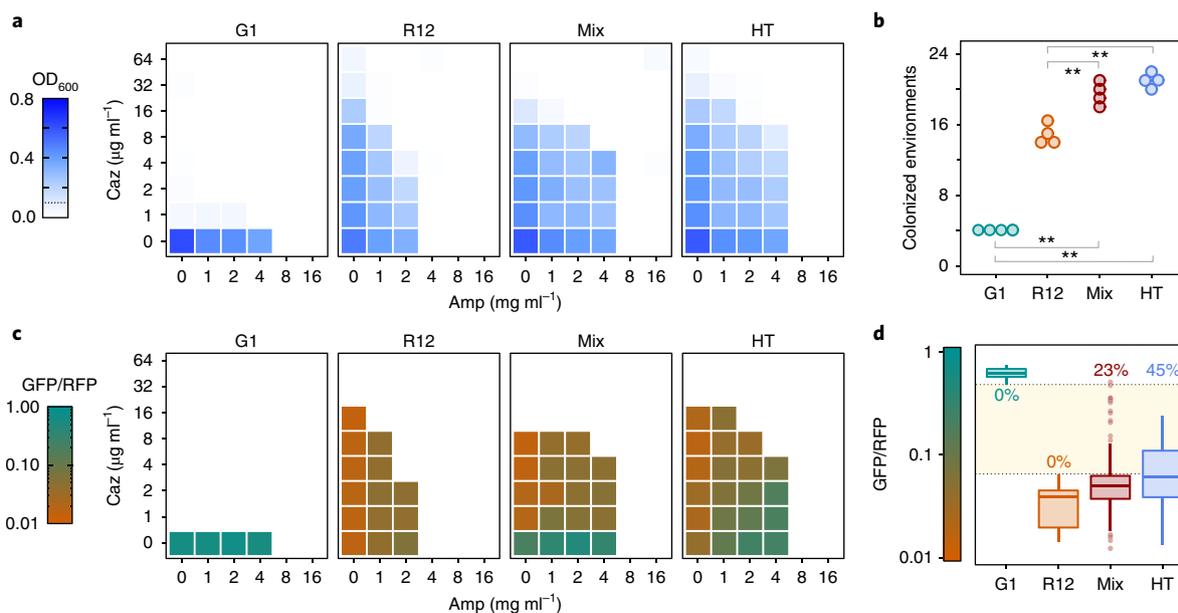
Fig. 2 | Bacterial growth and allelic content in the antibiotics array. a, The optical density (OD_{600}) of populations growing in a range of concentrations of Caz and Amp alone or in combination is colour-coded as indicated in the legend. We concluded that a particular environment in the array was colonized if, after 20 h of incubation, OD_{600} was greater than 0.1 (dotted line in the legend). **b**, The number of colonized environments of the four replicate arrays plotted for every genotype and the mixed population. The asterisks denote significant differences (Tukey's test $P < 0.001$ after significant ANOVA). **c**, The GFP/RFP fluorescence ratio (arbitrary units) offers insight into the allelic content of every environment and is plotted according the colour-code shown in the legend. **d**, Boxplots showing the distribution of fluorescence ratios in four replicate arrays for each genotype. The yellow-shaded region denotes fluorescence levels between those of the G1 and R12 strains and thus those populations carrying both plasmids at detectable levels. The numbers designate the percentage of environments colonized by a population containing both plasmids. For the sake of clarity only one of four replicates is shown in **a** and **c**. All four individual replicates can be found in Supplementary Data 1, under the label 'day 1'.
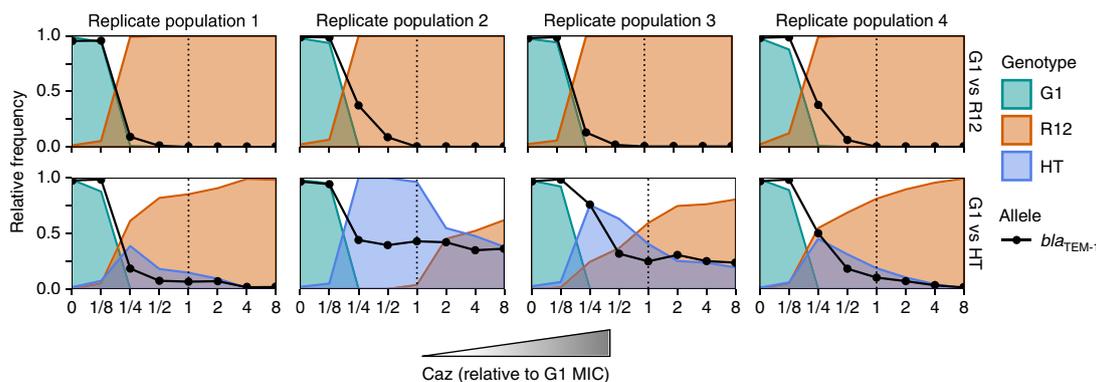

Fig. 3 | Invasion experiments. The upper panels show invasion experiments in which G1 population was invaded by a rare R12 population (1%); the lower panels show invasion experiments in which the HT strain invaded instead of R12. Experimental results obtained with four replicate populations (columns). Invasion experiments were carried out for eight consecutive days in which the Caz concentration in the medium was doubled daily. Each panel shows, for an individual invasion, the relative frequency of every genotype on each day, calculated by selective plating (filled areas). The solid black line shows the frequency of pBGT-1/pBRT-12 (bla_{TEM-1}/bla_{TEM-12}) calculated by qPCR. The black dotted vertical line denotes the day on which the MIC of Caz for G1 was reached.

of the G1 minimal inhibitory concentration; MIC). In the control invasions this meant the rapid fixation of the R12 genotype. However, in the HT invasions, the HT strain displaced G1 but never reached fixation as it was gradually replaced by R12 cells that emerged as segregants through intracellular fixation of pBRT-12. Even so, HT cells were still detectable at the end of the experiment (mean 14.8%; range 0.005–37.9%) after approximately 77 bacterial generations under increasing selective pressure for the bla_{TEM-12} allele. qPCR results confirmed that bla_{TEM-1} is maintained throughout the experiment when HT is invading. Interestingly, these results showed that

HT cells are able to maintain bla_{TEM-1} in the population well above the MIC of Caz conferred by this allele, increasing the allelic diversity of these populations throughout the experiment. This result is demonstrated by the fact that the Simpson diversity index calculated from qPCR data over the experiment is significantly higher when the invading strain is HT than when it is R12 (repeated-measures ANOVA invading genotype by time interaction $F_{7,21} = 4.767$, $P < 0.003$). Taken together, these results demonstrate that by slowing down the fixation of beneficial mutations multicopy plasmids preserve genetic diversity against strong selective pressures.
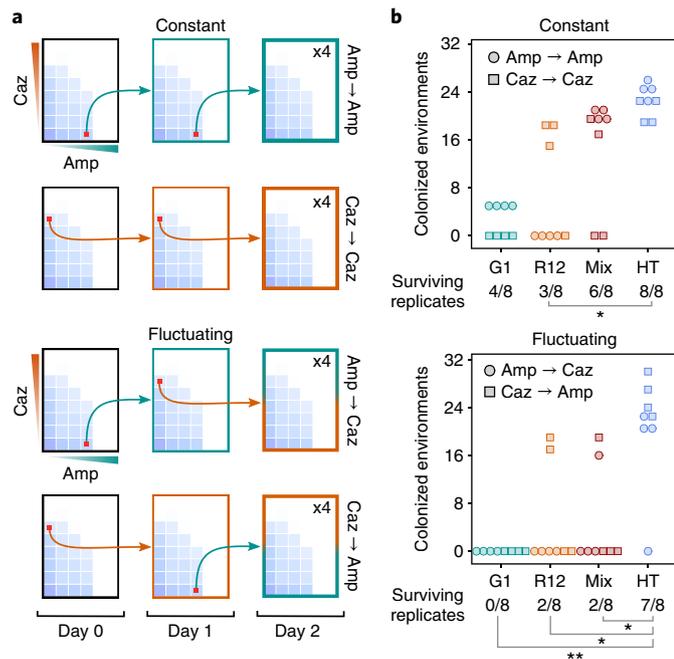
Fig. 4 | MCPs alleviate trade-offs under strong selective pressures.
a, Experimental design. Each plate represents an antibiotic array (identical to those shown in Fig. 2) from which the bacterial populations growing in either high Caz or high Amp concentrations (red filled squares) were diluted and used to sequentially seed new antibiotic arrays over a two-day course. This gives rise to four selective regimes; two in which selection was held constant (Caz → Caz and Amp → Amp) and two with fluctuating selection (Caz → Amp and Amp → Caz). **b**, Dot plot showing the number of colonized environments by each replicate line at the end of the experiment (day 2). Each dot represents a replicate line, and the symbol denotes the antibiotic treatment. Populations that became extinct colonized zero environments. Note that the results are grouped by the type of selection regimen. Under each panel, the number of surviving replicates is shown together with asterisks denoting statistical significance (*$P < 0.05$, **$P < 0.002$; χ^2 test). Raw data of all replicates can be found in Supplementary Data 1.

Multicopy plasmids promote adaptation under constant and fluctuating selective pressures. We have shown that MCPs allow populations to invade new environmental conditions and maintain genetic diversity over time in bacterial populations. These results suggest that MCPs may provide an important evolutionary advantage by alleviating trade-offs over time and promoting adaptation in bacterial populations under strong selective pressures. To test this possibility, we designed a short-term selection experiment in which we propagated G1, R12, HT and mixed populations (G1 + R12) under constant or fluctuating strong selective pressure with Amp ($4,096\,mg\,l^{-1}$) and Caz ($16\,mg\,l^{-1}$) over a period of two days (Fig. 4a). Although below the MIC, these concentrations are the highest at which growth of any of the genotypes was observed and therefore imposed an extremely stringent selective pressure for the bla_{TEM} alleles. This approach led to four possible antibiotic treatment routes that can be grouped into two constant selection regimes (Amp → Amp and Caz → Caz) and two fluctuating selection regimes (Amp → Caz and Caz → Amp). Every day, the populations able to survive the antibiotic treatments were inoculated into a fresh complete array of 48 Caz/Amp environments. With this experiment, we were able to measure two adaptive traits for each genotype: (i) survival under strong selective pressure and (ii) the ability to grow in 48 Caz/Amp environments after selection. We predicted that the HT
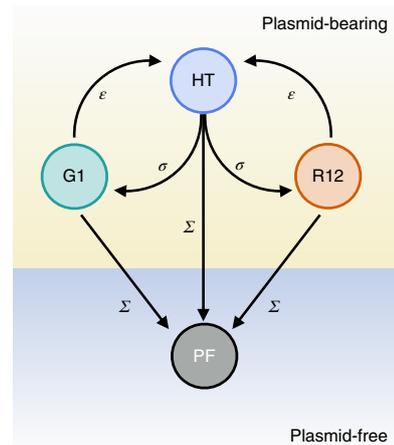

Fig. 5 | Theoretical model. Diagram illustrating the population dynamics of homozygote cells (G1 and R12), heterozygote cells (HT) and plasmid-free cells (PF). As described in the Methods, we assume that plasmids are uniformly distributed in the cell and therefore the rate of segregational loss (Σ) can be derived from the population-level mean plasmid copy number (see Methods and ref. [62]). Transitions between HT to G1 and R12 are also segregation-driven processes that occur at a rate σ, a parameter that can be estimated by assuming that HT cells have, in average, equal allelic proportions. The HT cells are produced by single-point mutation (occurring at a rate ε) in either G1 or R12 strains.

population would be able to escape trade-offs over time better that any other genotype, leading both to higher survival and to better colonization of Caz/Amp environments after the antibiotic treatments, especially under fluctuating selection regimes.

These predictions were confirmed with four experimental replicates for each genotype and treatment (Fig. 4b and Supplementary Data 1). The extinction patterns showed that although the HT strain was relatively insensitive to the antibiotic treatment, the homozygotes and the mixed populations faced massive extinctions. This pattern was especially true under fluctuating selection regimes, where all G1 replicates became extinct and only 2 of 8 replicate lines of the R12 homozygote population and 2 of 8 of the mixed population survived; in contrast, 7 of 8 HT strain replicates survived (HT versus Mix, HT versus R12 and HT versus G1; Fisher exact test $P < 0.04$). In addition, the surviving HT populations were able to colonize more environments at the end of the experiment than those from the homozygote and mixed populations regardless of the treatment (Tukey HSD $P < 0.00005$ after ANOVA effect of genotype on the number of colonized environments, $F = 25.116$, d.f. = 3, $P < 0.001$).

Given the short duration of the selection experiment, new antibiotic resistance mutations arising in the populations are unlikely. Hence, our results strongly suggest that the better survival of the HT strain and its markedly improved ability to thrive in the range of environments after selection are a consequence of the preservation of allelic richness by MCPs. Consistent with this view, we found that the HT strain maintained both alleles in a significantly higher number of environments than the mixed populations, both in constant regimes (35/181 versus 6/118 of colonized environments, respectively; $\chi^2 = 11.088$, d.f. = 1, $P < 0.001$) and in fluctuating regimes (57/167 versus 1/35; $\chi^2 = 12.341$, d.f. = 1, $P < 0.001$). Collectively, these results show that the maintenance of genetic diversity promoted by multicopy plasmids provides an evolutionary advantage in the colonization of new environments, especially when selective pressures rapidly shift.

Exploring the maintenance of plasmid-mediated heterozygosity under different selection regimes. A question that arises from our
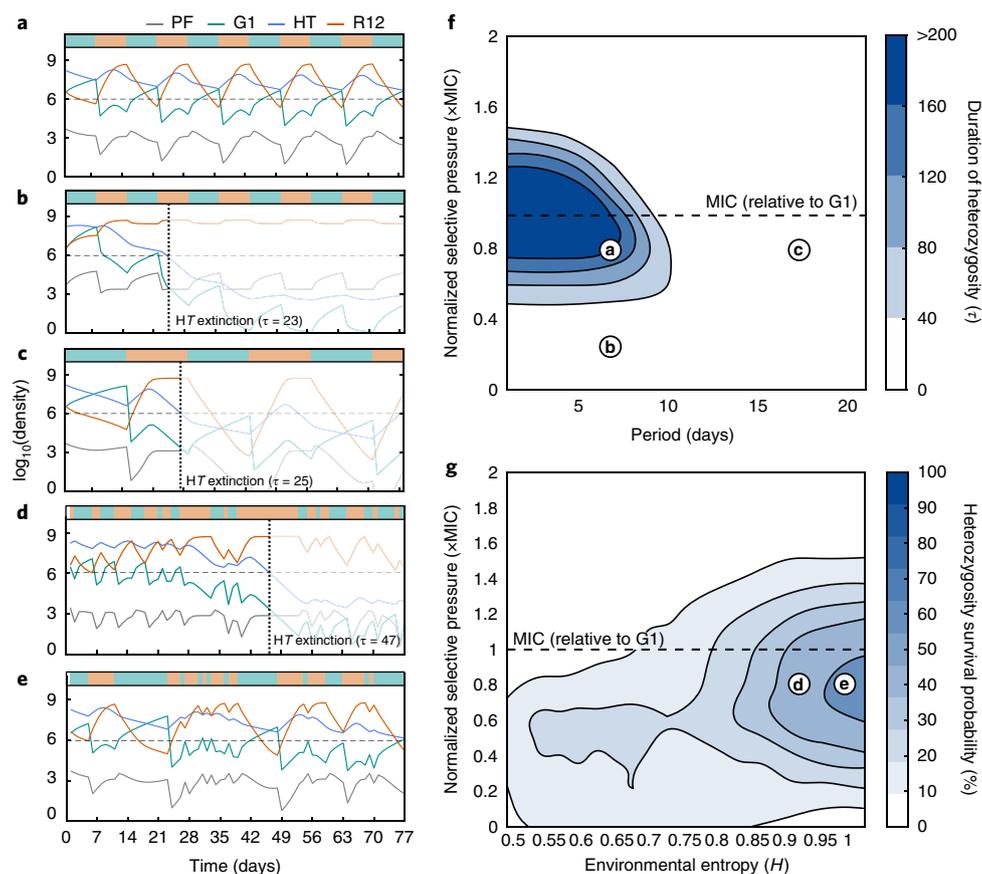
Fig. 6 | Numerical examples predicting the duration of plasmid-mediated heterozygosity under a range of fluctuating antibiotic conditions. **a–c**, Population dynamics in response to periodic selection regimes annotated in **f**. For clarity, only the densities at the end of each day are shown. **d–e**, Realizations of the model under the specific stochastic selection regimes annotated in **g**. **f**, Heat map representing the duration of heterozygosity under a range of normalized drug concentrations and periods of alternating drug exposure. Note how the regime **a** deploys drugs at 0.8×MIC in a seven-day period and is able to maintain the density of HT above the extinction threshold (in this case 10^6 cells). However, if the dose (as in regime **b**) or the frequency of environmental switching (as in regime **c**) is reduced, then the HT subpopulation is driven towards extinction. **g**, Heat map representing the survival probability of the HT population in response to different antibiotic concentrations and the entropy of the environment, a property that represents the uncertainty of each sequential treatment protocol.

work is to what extent plasmid-mediated heterozygosity (PMH) can be maintained in bacterial populations. As the homozygotes or plasmid-free cells will eventually replace the HT strain in any possible constant environment, PMH is inherently unstable. However, PMH may be stabilized in dynamic environments that alternately select for each allele, as in drug cycling protocols[23,24].

To test this possibility, we developed a simple compartmental population-dynamics model (Fig. 5) with parameter values obtained from experimental data (Methods and Supplementary Table 3). Our model accurately reproduces the evolutionary dynamics that emerge from the interaction between heterozygote and homozygote populations competing for limiting resources and exposed to the action of Caz and Amp (Supplementary Figs. 6,7). By systematically exploring a range of fluctuating environmental regimes, we obtained relevant statistics about the population dynamics that arise as a consequence of different patterns of selection.

First, we considered treatments that alternate periodically between Caz and Amp at normalized drug dosages (by adjusting the concentration of each drug so that they achieve equal inhibitory effect). We simulated a range of concentrations and periods of cycling and computed, for each selection regime, the time elapsed until the density of HT cells is less than the initial bacterial density, a value we refer to as duration of heterozygosity. The realizations of the model showed that PMH can last for hundreds of days under

regimes that present high frequencies of environmental switching and moderate drug concentrations (relative to the MIC of G1; Fig. 6).

However, fluctuations in nature are expected to be not periodic, but stochastic. To assess if the increased stability of PMH observed in periodic regimes is also present in stochastically switching environments, we generated $N = 10,000$ environmental regimes consisting of random sequences of both antibiotics. Each environmental regime is numerically generated by considering that the distribution of elapsed times between environmental switches follows an exponential distribution (see Methods). We also evaluated environmental regimes that randomly switched between three discrete states (Caz, Amp and a drug-free environment) and obtained qualitatively the same results. The Shannon entropy[25], H, of each previously determined environmental regime was used to quantify the uncertainty and stochasticity of each sequential treatment protocol. As shown in Fig. 6, environments with $H \ll 1$ have large single-drug time intervals that select for one of the homozygote strains and thus render PMH unstable. Conversely, duration of heterozygosity is maximized when exposed to selection regimes associated with high entropy values and moderate selective pressures (Supplementary Fig. 8).

Together, our computational study predicts that heterozygosity can be stabilized for relatively long periods of time in fluctuating environments with high temporal heterogeneity and intermediate selective pressures.

Discussion

In this study, we investigated the role of MCPs in the alleviation of trade-offs during evolutionary innovation in bacteria. We developed a traceable model system using plasmid-mediated bla_{TEM} genes that reproduces the evolutionary dynamics toward Caz resistance[21]. Our results demonstrate that the intrinsic properties of replication and segregation dynamics of MCPs allow bacterial populations to escape the restraints imposed by trade-offs on the colonization of new environments by facilitating the co-existence of the ancestral and evolved alleles within the same cell (Fig. 2). Critically, this co-existence was maintained over tens of generations in the presence of increasingly strong pressures for the evolved allele (Fig. 3), suggesting that MCPs are able to delay the loss of non-adaptive allelic variants and preserve allelic richness for generations. Allelic richness, in turn, translates into increased phenotypic robustness to withstand stringent fluctuating selective pressures (Fig. 4). Collectively, our experimental and theoretical models establish that when the evolution of the plasmid resident loci is constrained by fitness trade-offs, the heterozygote has an advantage compared to the homozygotes. Hence, the population is under balancing selection for the maintenance of both ancestral and evolved alleles, especially when the environments fluctuate[26]. Although examples of selection favouring heterozygotes are abundant[27,28], it comes as no surprise that these examples refer to polyploid eukaryotic organisms, in which new mutations are always heterozygous. In bacteria, MCP are able to provide heterozygote advantage because they represent an island of polyploidy in an otherwise haploid genome.

Previous studies have addressed the importance of MCPs in the evolution of new functions[21,29,30], and the co-existence of mutant and ancestral allele variants encoded in the same plasmid has recently been demonstrated in laboratory evolution experiments[21,31] and clinical settings[32]. However, the prevalence of plasmid-mediated heterozygosity in nature remains largely unknown. At least three arguments support the idea that plasmid-mediated heterozygosity could be pervasive in bacterial populations. First, natural MCPs encode important genes for bacterial physiology that are under strong selective forces such as antibiotic resistance genes[33], determinants of ecological interactions such as colicins[34], and even indispensable metabolic genes as in the aphid endosymbiont *Buchnera aphidicola*[35]. Second, MCPs are excellent platforms for the generation of genetic variation. Their multicopy nature increases the mutational supply and hence the chance of the resident loci acquiring mutations[21]. Additionally, this genetic variation can be further enriched by horizontal gene transfer[18] and inter- and intraplasmid recombination[36,37]. Third, MCPs are also excellent platforms for the preservation of genetic diversity. Our experimental results show that allelic richness can be maintained in the face of increasingly strong selective pressures for more than 75 bacterial generations, and our theoretical model indicates that it could be maintained for much longer periods under a range of conditions (Fig. 6 and Supplementary Fig. 10). Considering that natural *E. coli* populations are estimated to undergo 100–300 generations per year[38,39], we propose that the maintenance of genetic diversity by MCPs will persist long enough to profoundly affect bacterial evolvability. In view of these arguments, we predict that deep sequencing of bacterial clones (not populations) and careful examination of plasmid sequences from genomic data will increase the number of examples of plasmid-mediated heterozygosity in both experimental and natural scenarios.

Most plasmids cause a fitness cost to their host that should, in theory, constrain plasmid existence to very particular situations[40,41]. However, plasmids are extremely abundant in natural bacterial populations. This 'plasmid paradox' is particularly challenging in MCPs, as they lack mechanisms to increase their frequency such as active transfer or partitioning systems[42]. Several studies have offered compelling explanations for plasmid maintenance. For instance,

epistatic interactions have been shown to buffer plasmid cost[43,44]. Moreover, this cost can be ameliorated by compensatory mutations in either the plasmid or the bacterial chromosome[45–48]. Other possible explanations involve the increase in gene copies for the resident loci, which in turn translates into increased gene expression that could be beneficial under certain circumstances[21,35]. Our results raise the possibility that MCPs, as promoters of bacterial evolution, could be maintained by second-order selection, a process by which evolution indirectly selects for the systems that create adaptive mutations[49]. We propose that although the conditions for the maintenance of plasmids by second-order selection will be stringent, they are plausible in bacterial populations[49].

In conclusion, the ability of MCP-encoded genes to overcome the constraints imposed by trade-offs during evolutionary innovation could play a key role in the evolution of novel traits in bacterial populations and in the colonization of new environments. Additionally, our results may have implications for antibiotic therapies designed to slow the evolution of resistance by taking advantage of resistance trade-offs, such as drug cycling[24] or the exploitation of collateral sensitivity networks[50]. Future work will be needed to test the extent to which MCPs can jeopardize the success of these promising antimicrobial strategies.

Methods

Strains, media and plasmid construction. The plasmids used in this study (Supplementary Table 1) are derivatives of the pBGT and pBGT R164S plasmids that were previously used to reconstruct the plasmid-mediated evolution of Caz resistance[21]. For the sake of clarity, these plasmids were named pBGT-1 and pBGT-12 after the bla_{TEM} allele present. These plasmids also carry a *gfp* gene under the control of an L-arabinose inducible promoter, the gene coding for the repressor of this promoter *araC*, and a chloramphenicol (Chl) resistance acetyltransferase gene, *cat*. Variants of both plasmids in which the *gfp* gene was precisely replaced by the *dsRED* gene, encoding a red fluorescent protein, were generated by the Gibson assembly method[51] using the primers listed in Supplementary Table 2. To allow appropriate selection of heterozygote cells, a selective marker was needed to distinguish between plasmids. To this end, *cat* gene of the plasmids encoding bla_{TEM-12} was inactivated by creating an in-frame deletion (Δ574–591 in *cat* open reading frame) by site-directed mutagenesis using the primers $Cat_{SDM}F$ and $Cat_{SDM}R$ (Supplementary Table 2) and the Q5 Site-Directed Mutagenesis Kit (New England Biolabs) following manufacturer instructions. This deletion completely abolishes *cat* function by eliminating six essential amino acids[52] and renders the cells Chl sensitive. All possible combinations of the two bla_{TEM} alleles with both fluorescent markers were generated. All plasmids were introduced by transformation into chemically competent MG1655 cells giving rise to the strains shown in Supplementary Table 1. Transformants were selected in Chl (15 mg l⁻¹) or Caz (1 mg l⁻¹) for plasmids carrying bla_{TEM-1} and bla_{TEM-12}, respectively. To generate the heterozygote strains, two plasmids were simultaneously co-transformed and selected in both antibiotics. Transformants were checked by PCR using the primers listed in Supplementary Table 2 and examined by confocal microscopy (Leica TCS SP5 multispectral confocal system) after induction of the fluorescent reporters by incubating the samples in Lysogeny broth (LB) supplemented with 0.1% L-arabinose for 4 h. All strains were routinely grown in LB medium supplemented with the appropriate antibiotics at 37 °C.

In agreement with previous reports[21], all plasmid carriers showed a reduced growth rate compared with the plasmid-free strain although there were no significant differences among plasmid-bearing strains (Tukey's multiple comparison of means $P > 0.27$; see Supplementary Table 1). No significant differences in plasmid copy number (estimated by qPCR, see below) were found in the new constructs compared to G1 (Multiple comparisons of means, $P > 0.05$), discarding any confounding effect in the interpretation of the data. Furthermore, genomic DNA of all the strains was isolated using the Wizard genomic DNA purification kit (Promega), following the manufacturer's instructions. Whole genome sequencing was conducted at the Wellcome Trust Centre for Human Genetics using the Illumina HiSeq4000 platform. Possible mutations were predicted using the breseq 0.30.0 pipeline[53] and using MG1655 genome (NC_000913.3) and plasmid sequences as references. Whole genome sequencing discarded the presence of unexpected mutations in coding regions of the chromosome or the plasmids in all the strains used in this study.

Antibiotic array. The antibiotic array was prepared in 96 well flat-bottom plates (Falcon) using the checkerboard technique[54]. To diminish inter-plate variability, all plates were prepared in the same day from a single stock solution using a Liquidator 96 manual pipetting system (Mettler Toledo) and stored at −20 °C prior to use. All plates were used within a week and appropriate controls were included

to check antibiotic stability over time. Bacteria were inoculated at a final dilution of 1:2,000 and incubated for 20 h at 37 °C. After incubation, optical density at 600 nm (OD_{600}) was determined after strong shaking in a Synergy HTX microplate reader (Biotek). We interpreted that a particular environment of the array was colonized if, after incubation, OD_{600} was greater than 0.1. Appropriate samples were then collected to inoculate the next day's plate. At the end of the experiment, plasmid DNA from samples of the surviving populations was extracted (Accuprep plasmid mini extraction kit; Bioneer) and the possible presence of plasmid hybrids containing both bla_{TEM} alleles was discarded by gel electrophoresis of undigested and PvuI (New England Biolabs) digested plasmid extractions. To determine the fluorescence ratio (GFP/RFP), L-arabinose to a final concentration of 0.1% was added to each well to induce the expression of the fluorescent reporters present on the plasmids. After 4 h of incubation at 37 °C to allow protein expression, the plates were further incubated for 18 h at 4 °C. This step favours dsRED maturation, which is slower than that of GFP[55]. The GFP/RFP ratio was calculated by dividing green fluorescence (485/528 nm) over red fluorescence (540/590 nm) signals in a Synergy HTX microplate reader (Biotek). After collection of all data, the GFP/RFP ratio was rescaled between 0.01 and 1 to make the results more amenable to interpretation.

Competition and invasion experiments. Minimal inhibitory concentrations (MIC) of Caz and Amp were determined for every strain by the microdilution method following CLSI guidelines[56] (Supplementary Table 1). Pairwise competitions between strains carrying bla_{TEM-1} and bla_{TEM-12} alleles were performed in media containing sub-inhibitory Caz concentrations and without antibiotics. Briefly, overnight cultures were mixed 1:1 and diluted 1:2,000 in fresh media. After 20 h of incubation at 37 °C with shaking every 15 minutes in a Synergy HTX Multimode Reader (Biotek), appropriate dilutions were plated in LB agar plates containing Chl (15 mg l⁻¹) to select G1 and R1 strains or Caz (1 mg l⁻¹) to select G12 and R12 strains. The fitness of strains carrying bla_{TEM-12} relative to the strains carrying bla_{TEM-1} was determined using the formula:

$$W_{bla_{TEM-12}} = \frac{\ln(N_{final;bla_{TEM-12}}/N_{initial;bla_{TEM-12}})}{\ln(N_{final;bla_{TEM-1}}/N_{initial;bla_{TEM-1}})}$$

where $W_{bla_{TEM-12}}$ is the relative fitness of the bla_{TEM-12} bearing clone; $N_{initial;bla_{TEM-12}}$ and $N_{final;bla_{TEM-12}}$ are the numbers of bla_{TEM-12} cells before and after the competition, and $N_{initial;bla_{TEM-1}}$ and $N_{final;bla_{TEM-1}}$ are the numbers of cells carrying bla_{TEM-1} plasmids before and after the competition. The minimal selective concentration (MSC) of Caz, defined as the minimal antibiotic concentration that produces a detectable fitness benefit for the bla_{TEM-12} carrying strains[22], was used as starting concentration for the invasion experiments.

Invasion experiments were started by mixing overnight cultures of either HT or R12 and G1 strains at a 1:100 proportion in fresh LB. Immediately, the mixes were diluted 1:2,000 into 96-well flat-bottom plates (Falcon) containing 0.2 ml of fresh media supplemented with the MSC of Caz. A checkerboard pattern was used to avoid cross-well contamination. After 20 h of growth at 37 °C (approximately 11 bacterial generations per day), the cultures were further diluted 1:2,000 and inoculated into fresh media containing doubled antibiotic concentrations. Samples were plated in LB agar supplemented with either Caz (1 mg l⁻¹), Chl (15 mg l⁻¹) or Caz + Chl (1 mg l⁻¹ + 15 mg l⁻¹) to quantify the number of cells corresponding to each genotype in the competitions. To verify that the selective plating procedure was specific and to discard the presence of new mutations in the bla_{TEM-1} gene, we sequenced the bla_{TEM} allele of four independent clones per replicate obtained on Caz + Chl plates at day five using the primers shown in Supplementary Table 2. All chromatograms consistently showed a double peak (C + A) at the nucleotide 484 of the bla_{TEM} open reading frame assessing the presence of both bla_{TEM-1} and bla_{TEM-12} alleles in these clones. No other mutations were found. We additionally ruled out the possible presence of plasmid hybrids containing both bla_{TEM} alleles by digestion as described above. To assess allelic proportion, samples were also stored at −20 °C for subsequent qPCR analysis.

Quantification of plasmid copy number and allele frequencies. Quantitative polymerase chain reaction (qPCR) was used to determine relative plasmid copy number and allele frequency using an Applied Biosystems 7300 Real-Time PCR System and SYBR select master mix (Applied Biosystems). Specific primers for the pBGT plasmid backbone and the dxs chromosomal gene were used as previously described[21]. Additionally, specific primers for the gfp and $dsRED$ genes were developed. All primer sequences can be found in Supplementary Table 2. Samples were prepared as previously described[57]. Briefly, bacterial cultures were pelleted (9,000g, 1 min), resuspended in molecular biology grade water and boiled (95 °C, 10 min). After brief centrifugation to spin down cellular debris, samples of the supernatant were diluted and subsequently used as template. Amplification conditions were as follows: initial denaturation for 2 min at 95 °C, followed by 40 cycles of denaturation for 15 s at 95 °C, annealing and extension for 1 min at 60 °C. After the amplification was completed and to control for the specificity of the reaction, a melting curve analysis was performed by cooling the reaction to 60 °C and then heating slowly to 95 °C. Inter-run calibration samples were used to normalize the results from different plates of each qPCR. Relative copy number was

calculated using the $\Delta\Delta C_T$ method as previously described[58]. All reactions showed similar efficiency values (92.7–93.8%, $R^2 > 0.998$) and produced amplicons of similar size (112–114 b.p.). Control reactions were carried out to ensure that relative plasmid copy number was comparable when using pBGT or GFP and RFP targeting primers.

Calculation of Simpson's diversity index. When the relative abundance of each allele could be quantified by qPCR, Simpson's diversity index was used. Simpson's index gives the probability that two randomly selected alleles from the population are equal and can be calculated as $\sum (P_{bla_{TEM-1}}^2 + P_{bla_{TEM-12}}^2)$ were P_i represents the relative proportion of each alelle[59]. Simpson's diversity index is an integrative measure that takes into account both population richness and evenness. In preliminary experiments, the GFP/RFP fluorescence ratio was found to strongly correlate with the allelic ratio estimated by qPCR (Pearson's product-moment correlation $t = 26.103$, d.f. = 16, $R^2 = 0.977$, $P < 10^{-13}$; Supplementary Fig. 5), demonstrating that it can be used as a proxy to assess the proportion of each allele. However, direct interpolation of allelic proportions from fluorescence data demonstrated to be unreliable. Instead, we used a more conservative approach in which the presence of both alleles in a particular environment was assessed by simply determining if the GFP/RFP ratio was comprised between that of the homozygotes. In this way, allelic richness of an environment can be confidently determined. We note, however, that this method underestimates the real environmental richness as populations carrying a small number of one plasmid type would show undetectable levels of fluorescence. In that sense, for an environment to be classified as having both alleles, it must have substantial amounts of both plasmids. We argue that this is indeed a strength of this approach, because an environment must show some extent of allelic evenness to be cataloged as rich by our method.

Population-level plasmid dynamics model. The objective of our model is to study the population dynamics that emerge in response to different environmental concentrations of resource and multiple bactericidal antibiotics. First, we will assume that the bacterial population is composed of a plasmid-free subpopulation (with density at time t denoted by $B_{PF}(t)$), a subpopulation of heterozygote cells (with density represented by $B_{HT}(t)$) and homozygote subpopulations G1 and R12 (with densities represented with $B_{G1}(t)$ and $B_{R12}(t)$, respectively). We will consider that growth of each subpopulation depends on the environmental concentration of a limiting resource, $R(t)$, and therefore we can model growth rate of subpopulation i with a standard Monod term, $G_i(R(t)) = \rho_i U_i(R(t))$, where ρ_i is the metabolic efficiency of the cell and $U_i(R) = V_i R/(K_i + R)$ a sigmoidal resource uptake function characterized by parameters V_i, K_i denoting, respectively, the maximum growth rate and half-saturation constants of bacterial type i. In order to model the action of antibiotics (in this case drugs Amp and Caz, with an additive interaction and concentration represented by D^A and D^C respectively) we consider that the susceptibility of strain B_i to Amp and Caz can be modelled with killing rates κ_i^A and κ_i^C. Conversely, δ_i^A and δ_i^C denote the rates of drug inactivation by the degrading enzyme produced by bacterial type i.

Note that the plasmids used in this study replicate as monomers and do not possess any molecular mechanisms that increase its stability (for example, active partitioning or post-segregational killing mechanisms). Therefore, we can assume that plasmids are uniformly distributed in the cell at the moment of division and, as a result, the probability of a plasmid-bearing cell producing a plasmid-free cell through segregation can be described by a Poisson process and thus the rate of plasmid loss via segregation is approximated by $\Sigma = 2^{1-\mu}$, where μ denotes the mean plasmid copy number in the population[47,60]. Similarly, the probability of a heterozygote cell giving rise to a homozygote cell can be estimated by assuming that, in average, HT cells have equal fractions of both plasmids and thus the rate of heterozygosity loss can be written as $\sigma = 2^{1-\mu/2}$. Therefore, our model makes the critical assumption that HT cells carry equal proportions of each plasmid. Although this simplification may underestimate the complex distribution of intracellular allele frequencies, our model accurately reproduces the experimental results (Supplementary Figs. 6,7). In our experimental system, the mean per-cell plasmid copy number is 19 and therefore the rate of heterozygosity loss is 1/362 while the rate of plasmid loss is considerably lower, at 1/524,288. Finally, the evolutionary dynamics of the system considers that the transition from B_{G1} and B_{R12} into B_{HT} occurs at a rate $\varepsilon > 0$ representing the probability of a single-point mutation in the bla_{TEM-1} or bla_{TEM-12} locus.

In summary, the system of ordinary differential equations that describe the plasmid dynamics at a population-level can be written as:

$$\frac{d}{dt}R = -(U_{PF}(R)B_{PF} + U_{G1}(R)B_{G1} + U_{HT}(R)B_{HT} + U_{R12}(R)B_{R12}) \quad (1)$$

$$\frac{d}{dt}D^A = -D^A(\delta_{PF}^A B_{PF} + \delta_{G1}^A B_{G1} + \delta_{HT}^A B_{HT} + \delta_{R12}^A B_{R12}) \quad (2)$$

$$\frac{d}{dt}D^C = -D^C(\delta_{PF}^C B_{PF} + \delta_{G1}^C B_{G1} + \delta_{HT}^C B_{HT} + \delta_{R12}^C B_{R12}) \quad (3)$$

$$\frac{\mathrm{d}}{\mathrm{d}t}B_{\mathrm{PF}} = G_{\mathrm{PF}}(R)B_{\mathrm{PF}} + \Sigma\left(G_{\mathrm{G1}}(R)B_{\mathrm{G1}} + G_{\mathrm{HT}}(R)B_{\mathrm{HT}} + G_{\mathrm{R12}}(R)B_{\mathrm{R12}}\right)$$
$$- B_{\mathrm{PF}}(\kappa_{\mathrm{PF}}^{A}D^{A} + \kappa_{\mathrm{PF}}^{C}D^{C}) \tag{4}$$

$$\frac{\mathrm{d}}{\mathrm{d}t}B_{\mathrm{G1}} = (1-\varepsilon-\Sigma)G_{\mathrm{G1}}(R)B_{\mathrm{G1}} + \sigma G_{\mathrm{HT}}(R)B_{\mathrm{HT}} - B_{\mathrm{G1}}(\kappa_{\mathrm{G1}}^{A}D^{A} + \kappa_{\mathrm{G1}}^{C}D^{C}) \tag{5}$$

$$\frac{\mathrm{d}}{\mathrm{d}t}B_{\mathrm{HT}} = (1-\Sigma)G_{\mathrm{HT}}(R)B_{\mathrm{HT}} + \varepsilon\left(G_{\mathrm{G1}}(R)B_{\mathrm{G1}} + G_{\mathrm{R12}}(R)B_{\mathrm{R12}}\right)$$
$$- B_{\mathrm{HT}}(\kappa_{\mathrm{HT}}^{A}D^{A} + \kappa_{\mathrm{HT}}^{C}D^{C}) \tag{6}$$

$$\frac{\mathrm{d}}{\mathrm{d}t}B_{\mathrm{R12}} = (1-\varepsilon-\Sigma)G_{\mathrm{R12}}(R)B_{\mathrm{R12}} + \sigma G_{\mathrm{HT}}B_{\mathrm{HT}} - B_{\mathrm{R12}}(\kappa_{\mathrm{R12}}^{A}D^{A} + \kappa_{\mathrm{R12}}^{C}D^{C}) \tag{7}$$

with parameters values estimated using a parametrization approach that implements a Markov Chain Monte Carlo (MCMC) method with Metropolis–Hastings sampling. A similar Bayesian approach was published previously[47] and allows us to obtain maximum likelihood estimates for the specific affinity V_i/K_i and the resource conversion rate, ρ_i, from experimental growth curves of each strain grown in isolation (Supplementary Fig. 9 shows the MCMC diagnostics plots). The inhibition parameters of each strain were estimated using single-drug dose–response experiments. Numerical solutions of the system of equations (1)–(7) were obtained using standard ODE solvers in Matlab, with parameter values summarized in Supplementary Table 3.

Computational experiments in fluctuating environments. In order to numerically simulate an N-day experimental serial dilution protocol, we considered that each day ($0 \le n < N$) resources are replenished at the beginning of each season, that is $R_n(0) = R_0$. The initial bacterial density on the first day ($n = 0$) can be written as $B_0\Gamma$, where $B_0 = 1 \times 10^6$ denotes the total initial bacterial density and $\Gamma = (\gamma_{\mathrm{PF}}, \gamma_{\mathrm{G1}}, \gamma_{\mathrm{HT}}, \gamma_{\mathrm{R12}})$ a vector containing the initial relative frequencies of each strain and thus $\gamma_{\mathrm{PF}} + \gamma_{\mathrm{G1}} + \gamma_{\mathrm{HT}} + \gamma_{\mathrm{R12}} = 1$. For subsequent seasons, $n > 1$, we consider the initial population density of each subpopulation to be a function of the terminal condition of the previous season, that is $\eta(B_{\mathrm{PF}}(T), B_{\mathrm{G1}}(T), B_{\mathrm{HT}}(T), B_{\mathrm{R12}}(T))$, whereby $\eta = 0.01$ denotes the dilution parameter and $T = 24$ the duration of each season.

To quantify the stability of single-cell genetic diversity, we use the duration of heterozygosity, τ, defined as the time elapsed until the density of B_{HT} is below an extinction threshold, that is $\tau > 0$ such that $B_{\mathrm{HT}}(\tau) < B_{\mathrm{ext}} = 1 \times 10^6$ and $B_{\mathrm{HT}}(t) \ge B_{\mathrm{ext}}$ for all $t \in [0, \tau)$. In particular, we considered fluctuating environmental regimes that alternate selection between both drugs, so if $\hat{D}^A$ and $\hat{D}^C$, represent the concentrations of each drug normalized to achieve equal inhibitory effect then on day n we can represent the treatment used as $D_n = \phi_n\hat{D}^A + (1-\phi_n)\hat{D}^C$. Here, we used $\phi_n = 0$ or $\phi_n = 1$ and therefore the environmental regime could be represented as a random sequence of N bits, allowing us to compute the information entropy (Shannon–Wiener Index) associated with each environmental sequence using the following expression: $H = -\sum P\log_2(P)$ where P represents the proportion of days where each drug was used. Note that low-values of H correspond to constant, predictable environments, whereas high entropy values are associated with unpredictable, rapidly switching environmental conditions.

The $bla_{\mathrm{TEM-1}}/bla_{\mathrm{TEM-12}}$ trade-off explored in this work can be considered 'weak' in the sense that the gain in the new function is big (64-fold increase in Caz MIC), whereas the loss in the ancestral function is small (twofold reduction in Amp MIC). In natural and laboratory evolution most trade-offs are weak[2] (>10-fold gain in new function versus loss of the existing one) and hence the trade-off of TEM evolution used in this work can be deemed representative. Nevertheless, we decided to theoretically explore various trade-off strengths to extend our computational analysis to other possible scenarios. As can be seen in Supplementary Fig. 10, stronger trade-offs increase the range of fluctuations and antibiotic pressures that render PMH stable. In contrast weaker trade-offs render PMH unstable in most conditions, as the acquisition of a new genetic activity barely involves any loss in the ancestral function.

Statistical analysis. Analyses were performed using R (v. 3.4.2)[61]. One way ANOVA and Tukey's multiple comparison of means were used to assess differences in colonization in the antibiotic array. Spearman's rank correlation coefficient was used to assess the monotonic relationship between antibiotic concentrations and the GFP/RFP ratio. A chi-squared (χ^2) test was used to analyse the frequency of populations conserving both alleles after growth in the antibiotic array. Repeated-measures ANOVA was used to ascertain the variation of Simpson's allelic diversity index over time in the invasion experiments. Fisher's exact test was used to analyse the differences in survival in the short-term selection experiment. A two-tailed two-sample t-test with Bonferroni correction was used to compare fitness data.

Pearson's product-moment correlation was used to assess the linear relationship between fluorescence and plasmid proportion determined by qPCR.

References

1. Conant, G. C. & Wolfe, K. H. Turning a hobby into a job: how duplicated genes find new functions. *Nat. Rev. Genet.* **9**, 938–950 (2008).
2. Khersonsky, O. & Tawfik, D. S. Enzyme promiscuity: a mechanistic and evolutionary perspective. *Annu. Rev. Biochem.* **79**, 471–505 (2010).
3. Toll-Riera, M., San Millan, A., Wagner, A. & MacLean, R. C. The genomic basis of evolutionary innovation in *Pseudomonas aeruginosa*. *PLoS Genet.* **12**, 1–21 (2016).
4. Childers, W. S. et al. Cell fate regulation governed by a repurposed bacterial histidine kinase. *PLoS Biol.* **12**, e1001979 (2014).
5. Anderson, D. P. et al. Evolution of an ancient protein function involved in organized multicellularity in animals. *eLife* **5**, e10147 (2016).
6. Bershtein, S. & Tawfik, D. S. Ohno's model revisited: measuring the frequency of potentially adaptive mutations under various mutational drifts. *Mol. Biol. Evol.* **25**, 2311–2318 (2008).
7. Stiffler, M. A., Hekstra, D. R. & Ranganathan, R. Evolvability as a function of purifying selection in TEM-1 β-lactamase. *Cell* **160**, 882–892 (2015).
8. Soskine, M. & Tawfik, D. S. Mutational effects and the evolution of new protein functions. *Nat. Rev. Genet.* **11**, 572–582 (2010).
9. Innan, H. & Kondrashov, F. The evolution of gene duplications: classifying and distinguishing between models. *Nat. Rev. Genet.* **11**, 97–108 (2010).
10. Andersson, D. I. & Hughes, D. Gene amplification and adaptive evolution in bacteria. *Annu. Rev. Genet.* **43**, 167–195 (2009).
11. Bergthorsson, U., Andersson, D. I. & Roth, J. R. Ohno's dilemma: evolution of new genes under continuous selection. *Proc. Natl Acad. Sci. USA* **104**, 17004–17009 (2007).
12. Pettersson, M. E., Sun, S., Andersson, D. I. & Berg, O. G. Evolution of new gene functions: simulation and analysis of the amplification model. *Genetica* **135**, 309–324 (2009).
13. Adler, M., Anjum, M., Berg, O. G., Andersson, D. I. & Sandegren, L. High fitness costs and instability of gene duplications reduce rates of evolution of new genes by duplication-divergence mechanisms. *Mol. Biol. Evol.* **31**, 1526–1535 (2014).
14. Sandegren, L. & Andersson, D. I. Bacterial gene amplification: implications for the evolution of antibiotic resistance. *Nat. Rev. Microbiol.* **7**, 578–588 (2009).
15. Toussaint, J.-P. et al. Gene duplication in *Pseudomonas aeruginosa* improves growth on adenosine. *J. Bacteriol.* **199**, e00261-17 (2017).
16. Näsvall, J., Sun, L., Roth, J. R. & Andersson, D. I. Real-time evolution of new genes by innovation, amplification, and divergence. *Science* **338**, 384–387 (2012).
17. Stoesser, N. et al. Evolutionary history of the global emergence of the *Escherichia coli* epidemic clone ST131. *mBio* **7**, e02162 (2016).
18. Summers, D. K. *The Biology of Plasmids* (Blackwell, 2009).
19. Mroczkowska, J. E. & Barlow, M. Fitness trade-offs in blaTEM evolution. *Antimicrob. Agents Chemother.* **52**, 2340–2345 (2008).
20. Schenk, M. F. et al. Role of pleiotropy during adaptation of TEM-1 β-lactamase to two novel antibiotics. *Evol. Appl.* **8**, 248–260 (2015).
21. San Millan, A., Escudero, J. A., Gifford, D. R., Mazel, D. & MacLean, R. C. Multicopy plasmids potentiate the evolution of antibiotic resistance in bacteria. *Nat. Ecol. Evol.* **1**, 0010 (2016).
22. Gullberg, E. et al. Selection of resistant bacteria at very low antibiotic concentrations. *PLoS Pathog.* **7**, e1002158 (2011).
23. Fuentes-Hernandez, A. et al. Using a sequential regimen to eliminate bacteria at sublethal antibiotic dosages. *PLoS Biol.* **13**, e1002104 (2015).
24. Kim, S., Lieberman, T. D. & Kishony, R. Alternating antibiotic treatments constrain evolutionary paths to multidrug resistance. *Proc. Natl Acad. Sci. USA* **111**, 14494–14499 (2014).
25. Shannon, C. E. A mathematical theory of communication. *Bell Syst. Tech. J.* **27**, 623–656 (1948).
26. Charlesworth, D. Balancing selection and its effects on sequences in nearby genome regions. *PLoS Genet.* **2**, 379–384 (2006).
27. Sellis, D., Kvitek, D. J., Dunn, B., Sherlock, G. & Petrov, D. A. Heterozygote advantage is a common outcome of adaptation in *Saccharomyces cerevisiae*. *Genetics* **203**, 1401–1413 (2016).

28. Niskanen, A. K. et al. Balancing selection and heterozygote advantage in major histocompatibility complex loci of the bottlenecked Finnish wolf population. *Mol. Ecol.* **23**, 875–889 (2014).

29. Holloway, A. K., Palzkill, T. & Bull, J. J. Experimental evolution of gene duplicates in a bacterial plasmid model. *J. Mol. Evol.* **64**, 215–222 (2007).

30. Dhar, R., Bergmiller, T. & Wagner, A. Increased gene dosage plays a predominant role in the initial stages of evolution of duplicate tem-1 beta lactamase genes. *Evolution* **68**, 1775–1791 (2014).

31. Bedhomme, S., Perez Pantoja, D. & Bravo, I. G. Plasmid and clonal interference during post horizontal gene transfer evolution. *Mol. Ecol.* **26**, 1832–1847 (2017).

32. Santos-Lopez, A. et al. A naturally occurring SNP in plasmid pB1000 produces a reversible increase in antibiotic resistance. *Antimicrob. Agents Chemother.* **2**, AAC.01735-16 (2016).

33. Wu, P. J., Shannon, K. & Phillips, I. Mechanisms of hyperproduction of TEM-1 beta-lactamase by clinical isolates of *Escherichia coli*. *J. Antimicrob. Chemother.* **36**, 927–939 (1995).

34. Cascales, E. et al. Colicin biology. *Microbiol. Mol. Biol. Rev.* **71**, 158–229 (2007).

35. Latorre, A., Gil, R., Silva, F. J. & Moya, A. Chromosomal stasis versus plasmid plasticity in aphid endosymbiont *Buchnera aphidicola*. *Heredity* **95**, 339–347 (2005).

36. Gomez, A. et al. Creating new genes by plasmid recombination in *Escherichia coli* and *Bacillus subtilis*. *Appl. Environ. Microbiol.* **71**, 7607–7609 (2005).

37. Rodríguez-Beltrán, J. et al. High recombinant frequency in extraintestinal pathogenic *Escherichia coli* strains. *Mol. Biol. Evol.* **32**, 1708–1716 (2015).

38. Guttman, D. S. & Dykhuizen, D. E. Clonal divergence in *Escherichia coli* as a result of recombination, not mutation. *Science* **266**, 1380–1383 (1994).

39. Gibbons, R. J. & Kapsimalis, B. Estimates of the overall rate of growth of the intestinal microflora of hamsters, guinea pigs, and mice. *J. Bacteriol.* **93**, 510–512 (1967).

40. Vogwill, T. & Maclean, R. C. The genetic basis of the fitness costs of antimicrobial resistance: a meta-analysis approach. *Evol. Appl.* **8**, 284–295 (2015).

41. San Millan, A. & MacLean, R. C. Fitness costs of plasmids: a limit to plasmid transmission. *Microbiol. Spectr.* **5**, 5 (2017).

42. Smillie, C., Garcillán-Barcia, M. P., Francia, M. V., Rocha, E. P. C. & de la Cruz, F. Mobility of plasmids. *Microbiol. Mol. Biol. Rev.* **74**, 434–452 (2010).

43. San Millan, A., Heilbron, K. & MacLean, R. C. Positive epistasis between co-infecting plasmids promotes plasmid survival in bacterial populations. *ISME J.* **8**, 601–612 (2014).

44. Silva, R. F. et al. Pervasive sign epistasis between conjugative plasmids and drug-resistance chromosomal mutations. *PLoS Genet.* **7**, e1002181 (2011).

45. Harrison, E. et al. Parallel compensatory evolution stabilizes plasmids across the parasitism–mutualism continuum. *Curr. Biol.* **25**, 2034–2039 (2015).

46. Porse, A., Schønning, K., Munck, C. & Sommer, M. O. A. Survival and evolution of a large multidrug resistance plasmid in new clinical bacterial hosts. *Mol. Biol. Evol.* **33**, 2860–2873 (2016).

47. San Millan, A. et al. Positive selection and compensatory adaptation interact to stabilize non-transmissible plasmids. *Nat. Commun.* **5**, 5208 (2014).

48. Loftie-Eaton, W. et al. Compensatory mutations improve general permissiveness to antibiotic resistance plasmids. *Nat. Ecol. Evol.* **1**, 1354–1363 (2017).

49. Tenaillon, O., Taddei, F., Radman, M. & Matic, I. Second-order selection in bacterial evolution: selection acting on mutation and recombination rates in the course of adaptation. *Res. Microbiol.* **152**, 11–16 (2001).

50. Imamovic, L. & Sommer, M. O. A. Use of collateral sensitivity networks to design drug cycling protocols that avoid resistance development. *Sci. Transl. Med.* **5**, 204ra132 (2013).

51. Gibson, D. G. et al. Enzymatic assembly of DNA molecules up to several hundred kilobases. *Nat. Methods* **6**, 343–345 (2009).

52. Leslie, A. G., Moody, P. C. & Shaw, W. V. Structure of chloramphenicol acetyltransferase at 1.75-A resolution. *Proc. Natl Acad. Sci. USA* **85**, 4133–4137 (1988).

53. Deatherage, D. E. & Barrick, J. E. Identification of mutations in laboratory-evolved microbes from next-generation sequencing data using breseq. *Methods Mol. Biol.* **1151**, 165–188 (2014).

54. Bonapace, C. R., Bosso, J. A., Friedrich, L. V. & White, R. L. Comparison of methods of interpretation of checkerboard synergy testing. *Diagn. Microbiol. Infect. Dis.* **44**, 363–366 (2002).

55. Gross, L. A., Baird, G. S., Hoffman, R. C., Baldridge, K. K. & Tsien, R. Y. The structure of the chromophore within DsRed, a red fluorescent protein from coral. *Proc. Natl Acad. Sci. USA* **97**, 11990–11995 (2000).

56. *Performance Standards for Antimicrobial Susceptibility Testing; Twenty-Fourth Informational Supplement* (Clininical and Laboratory Standards Institute, 2014).

57. Skulj, M. et al. Improved determination of plasmid copy number using quantitative real-time PCR for monitoring fermentation processes. *Microb. Cell Fact.* **7**, 6 (2008).

58. Livak, K. J. & Schmittgen, T. D. Analysis of relative gene expression data using real-time quantitative PCR and the $2-\Delta\Delta CT$ method. *Methods* **25**, 402–408 (2001).

59. Jost, L. Entropy and diversity. *Oikos* **113**, 363–375 (2006).

60. Summers, D. K. The kinetics of plasmid loss. *Trends Biotechnol.* **9**, 273–278 (1991).

61. R Core Team *R: A Language and Environment for Statistical Computing* (R Foundation for Statistical Computing, Vienna, 2017).

62. Levin, B. R. & Stewart, F. M. The population biology of bacterial plasmids: a priori conditions for the existence of mobilizable nonconjugative factors. *Genetics* **94**, 425–443 (1980).

Acknowledgements

Author contributions

J.R.B., A.S.M. and R.C.M. were responsible for the conceptualization of the study; J.R.B., A.S.M. and J.A.E. designed the methodology; R.P.M., J.C.R.H.B. and A.F.H. postulated and analysed the mathematical model; J.C.R.H.B., A.F.H., J.A.E., J.D. and J.R.B. performed experiments and contributed to data analysis; J.R.B. and A.S.M. analysed data and prepared the original draft of the manuscript and undertook the reviewing and editing; all authors supervised and approved the final version of the manuscript. A.S.M. was responsible for funding acquisition and supervision.

Competing interests

The authors declare no competing interests.

Additional information

Supplementary information is available for this paper at https://doi.org/10.1038/s41559-018-0529-z.

Reprints and permissions information is available at www.nature.com/reprints.

Correspondence and requests for materials should be addressed to J.R. or A.S.

Publisher's note: Springer Nature remains neutral with regard to jurisdictional claims in published maps and institutional affiliations.

naturereasearch

Corresponding author(s): Alvaro San Millan & Jeronimo Rodriguez-Beltran

Life Sciences Reporting Summary

Nature Research wishes to improve the reproducibility of the work that we publish. This form is intended for publication with all accepted life science papers and provides structure for consistency and transparency in reporting. Every life science submission will use this form; some list items might not apply to an individual manuscript, but all fields must be completed for clarity.

For further information on the points included in this form, see Reporting Life Sciences Research. For further information on Nature Research policies, including our data availability policy, see Authors & Referees and the Editorial Policy Checklist.

Please do not complete any field with "not applicable" or n/a. Refer to the help text for what text to use if an item is not relevant to your study.
For final submission: please carefully check your responses for accuracy; you will not be able to make changes later.

▶ Experimental design

1. Sample size

   Describe how sample size was determined.

   > The maximum number of replicates that were experimentally feasible was used.

2. Data exclusions

   Describe any data exclusions.

   > No data was excluded from the analysis.

3. Replication

   Describe the measures taken to verify the reproducibility of the experimental findings.

   > All attempts at replication were successful and are included in the manuscript.

4. Randomization

   Describe how samples/organisms/participants were allocated into experimental groups.

   > Bacterial replicates of different strains were randomly allocated in multi-well plates to avoid position and inter-plate effects for experiments in Figures 2, 3 & 4.

5. Blinding

   Describe whether the investigators were blinded to group allocation during data collection and/or analysis.

   > NA

   Note: all in vivo studies must report how sample size was determined and whether blinding and randomization were used.

6. Statistical parameters

   For all figures and tables that use statistical methods, confirm that the following items are present in relevant figure legends (or in the Methods section if additional space is needed).

n/a	Confirmed	
☐	☒	The exact sample size (n) for each experimental group/condition, given as a discrete number and unit of measurement (animals, litters, cultures, etc.)
☐	☒	A description of how samples were collected, noting whether measurements were taken from distinct samples or whether the same sample was measured repeatedly
☐	☒	A statement indicating how many times each experiment was replicated
☐	☒	The statistical test(s) used and whether they are one- or two-sided *Only common tests should be described solely by name; describe more complex techniques in the Methods section.*
☐	☒	A description of any assumptions or corrections, such as an adjustment for multiple comparisons
☐	☒	Test values indicating whether an effect is present *Provide confidence intervals or give results of significance tests (e.g. P values) as exact values whenever appropriate and with effect sizes noted.*
☐	☒	A clear description of statistics including central tendency (e.g. median, mean) and variation (e.g. standard deviation, interquartile range)
☐	☒	Clearly defined error bars in all relevant figure captions (with explicit mention of central tendency and variation)

See the web collection on statistics for biologists for further resources and guidance.

▶ Software

Policy information about availability of computer code

7. Software

Describe the software used to analyze the data in this study.

> The data was analyzed using R statistical programming

For manuscripts utilizing custom algorithms or software that are central to the paper but not yet described in the published literature, software must be made available to editors and reviewers upon request. We strongly encourage code deposition in a community repository (e.g. GitHub). *Nature Methods* guidance for providing algorithms and software for publication provides further information on this topic.

▶ Materials and reagents

Policy information about availability of materials

8. Materials availability

Indicate whether there are restrictions on availability of unique materials or if these materials are only available for distribution by a third party.

> All materials are available from the authors under request

9. Antibodies

Describe the antibodies used and how they were validated for use in the system under study (i.e. assay and species).

> No antiboidies were used

10. Eukaryotic cell lines

a. State the source of each eukaryotic cell line used.

> No eukaryotic cell lines were used

b. Describe the method of cell line authentication used.

> NA

c. Report whether the cell lines were tested for mycoplasma contamination.

> NA

d. If any of the cell lines used are listed in the database of commonly misidentified cell lines maintained by ICLAC, provide a scientific rationale for their use.

> NA

▶ Animals and human research participants

Policy information about studies involving animals; when reporting animal research, follow the ARRIVE guidelines

11. Description of research animals

Provide all relevant details on animals and/or animal-derived materials used in the study.

> No research animals were used

Policy information about studies involving human research participants

12. Description of human research participants

Describe the covariate-relevant population characteristics of the human research participants.

> Our study does not involve human research